THE JOURNAL OF BIOLOGICAL CHEMISTRY VOL. 286, NO. 13, pp. 11875–11882, April 1, 2011

Natural Loss-of-function Mutation of Myeloid Differentiation Protein 88 Disrupts Its Ability to Form Myddosomes

Received for publication, November 1, 2010, and in revised form, February 7, 2011 Published, JBC Papers in Press, February 16, 2011, DOI 10.1074/jbc.M110.199653

Kamalpreet Nagpal[‡1], Theo S. Plantinga[§], Cherilyn M. Sirois[‡], Brian G. Monks[‡], Eicke Latz[‡¶], Mihai G. Netea[§2], and Douglas T. Golenbock[‡1,3]

From the [‡]Division of Infectious Diseases and Immunology, Department of Medicine, University of Massachusetts Medical School, Worcester, Massachusetts 01605, the [§]Department of Medicine and Nijmegen Institute for Infection, Inflammation, and Immunity, Radboud University Nijmegen Medical Center, 6500 HD Nijmegen, The Netherlands, and the [¶]Institute of Innate Immunity, University of Bonn, 53127 Bonn, Germany

Myeloid differentiation protein 88 (MyD88) is a key signaling adapter in Toll-like receptor (TLR) signaling. MyD88 is also one of the most polymorphic adapter proteins. We screened the reported nonsynonymous coding mutations in MyD88 to identify variants with altered function. In reporter assays, a death domain variant, S34Y, was found to be inactive. Importantly, in reconstituted macrophage-like cell lines derived from knockout mice, MyD88 S34Y was severely compromised in its ability to respond to all MyD88-dependent TLR ligands. Unlike wild-type MyD88, S34Y is unable to form distinct foci in the cells but is present diffused in the cytoplasm. We observed that IRAK4 co-localizes with MyD88 in these aggregates, and thus these foci appear to be "Myddosomes." The MyD88 S34Y loss-of-function mutant demonstrates how proper cellular localization of MyD88 to the Myddosome is a feature required for MyD88 function.

Toll-like receptors (TLRs)[4] are a part of the innate immune system and play a critical role in host defense against a variety of pathogens. Ten functional TLRs in humans and 12 in mice have been identified to date (1). Each TLR recognizes different categories of evolutionarily conserved patterns called pathogen-associated molecular patterns in microbes. For example, TLR4 recognizes lipopolysaccharide (LPS) from the cell walls of bacteria, whereas CpG-rich DNA from bacteria and viruses acts as the ligand for TLR9.

Much of the diversity of TLR pathways can be attributed to differential use of the TIR domain-containing adapter proteins. There are four adapter proteins: MyD88, MyD88 adapter-like (Mal), also called TIR domain-containing adapter protein (TIRAP), TIR domain-containing adapter-inducing interferon-β (TRIF), and TRIF-related adaptor molecule (TRAM). MyD88 is a key adapter protein involved in signaling from all of the TLRs except TLR3 and the TRIF-mediated arm of TLR4 signaling. Thus, depending on its use, TLR pathways can be divided into MyD88-dependent and MyD88-independent pathways. The engagement of a particular TLR by its ligand triggers a signaling cascade, which culminates in the secretion of various proinflammatory cytokines and interferons.

MyD88 is a 296-amino acid protein with a modular domain structure. In addition to the N-terminal TIR domain, it has a death domain at its C terminus. The crystal structure of the MyD88 death domain has recently been resolved, and it reveals that MyD88 exists in oligomeric form in solution (2). These oligomers of MyD88 can recruit the death domains of interleukin-1 receptor-associated kinase (IRAK)4 and IRAK2 to form a ternary complex called the Myddosome.

The importance of single nucleotide polymorphisms (SNPs) in TLR-related proteins has recently been brought to the forefront, with many studies implicating SNPs in disease susceptibility and outcome (3–7). Mal and MyD88 are the most polymorphic of the four adapter proteins, and Mal has received the most scrutiny in this regard (8–10). However, other than a study by Von Bernuth *et al.*, where children with MyD88 deficiencies were shown to have recurrent pyogenic bacterial infections (11), studies on MyD88 variants have been scarce. The central role of MyD88 in TLR signaling thus warrants a deeper understanding of the effects of SNPs on the activity/function of MyD88.

In this study we have screened the six nonsynonymous polymorphisms in the coding region of MyD88 with the aim of identifying polymorphisms that alter the function of MyD88. We identify and characterize a death domain variant, S34Y, that is completely inactive in all MyD88-dependent TLR signaling. We further show that this mutant has a localization pattern different from that of wild-type (WT) MyD88 and is unable to form Myddosomes with IRAK4 and IRAK2.

EXPERIMENTAL PROCEDURES

Plasmids and Site-directed Mutagenesis—The plasmids pEFBOS-MyD88-HA (12), pCMV-IRF5-FLAG (13), NF-κB luciferase, interferon-stimulated response element (ISRE) luciferase, and *Renilla* luciferase (14), and the retroviral vector pMSCV2.2-IRES-GFP (15) have been described elsewhere. The different variants of MyD88 (in pEFBOS-MyD88-HA and pMSCV2.2-ISRE-GFP background) were generated by using

[1] Supported by National Institutes of Health Grants AI084048 and GM54060.
[2] Supported by a Vici grant from The Netherlands Organization for Scientific Research.
[3] To whom correspondence should be addressed. Tel.: 508-856-5980; Fax: 508-856-5463; E-mail: douglas.golenbock@umassmed.edu.
[4] The abbreviations used are: TLR, Toll-like receptor; IRAK, interleukin-1 receptor-associated kinase; IRES, internal ribosomal entry sequence; IRF, interferon response factor; ISRE, interferon-stimulated response element; Mal, MyD88 adapter-like; MyD88, myeloid differentiation protein 88; SE, sensitized emission; TIRAP, TIR domain containing adapter protein; TRIF, TIR domain-containing adapter-inducing interferon-β; TIR, Toll interleukin-1 receptor.

the QuikChange site-directed mutagenesis kit (Stratagene) according to the manufacturer's instructions. Cerulean-tagged IRAK4 and citrine-tagged MyD88 were cloned into a vector that was modified from the original pCLXSN backbone from Imgenex (16). All of the expression constructs were verified by sequencing.

Luciferase Reporter Assay—HEK293T cells were seeded in a 96-well plate at a density of 20,000 cells/well and transfected the next day with either NF-κB or ISRE luciferase reporter (40 ng), *Renilla* reporter (40 ng), and the indicated amounts of either pEFBOS-MyD88 (WT) or the different variants using Genejuice (EMD Biosciences, San Diego, CA). In the case of the ISRE reporter assay, interferon response factor 5 (IRF5) (5 ng) was co-transfected. Twenty-four hours after transfection, reporter gene activity was measured using the Dual Luciferase Assay System (Promega). The thymidine kinase *Renilla* luciferase reporter values were used to normalize the data for transfection efficiency.

Retroviral Transduction of Immortalized Macrophage-like Cell Lines—The immortalized MyD88-deficient macrophage-like cell line has been described elsewhere (17). The retroviral vector MSCV2.2 (15) carrying either HA-tagged WT MyD88 or MyD88 S34Y was used to transduce MyD88-deficient cells. This retrovirus transcribes GFP from an internal ribosomal entry sequence (IRES) element. The positive cells were thus sorted based on GFP expression, and the expression of the MyD88 proteins was compared by immunoblotting with anti-HA antibody.

Enzyme-linked Immunosorbent Assay—WT, MyD88-deficient, and MyD88-deficient cells expressing WT MyD88 or MyD88 S34Y were seeded into 96-well plates at a density of 25,000 cells/well and stimulated overnight with TLR ligands at the indicated concentrations. TNF-α in the supernatants was measured using ELISA kits from R&D Systems according to the manufacturer's instructions. The same supernatants were also assessed for IFN-β levels as described (18).

IκB-α Degradation and MAPK Activation Assays—WT, MyD88-deficient, and MyD88-deficient cells expressing WT MyD88 or MyD88 S34Y were seeded into a 6-well plate at a density of 2×10^6 cells/well. The next day, the cells were stimulated with either PAM_2CSK_4 (10 nM) or R848 (20 μM) for the indicated time intervals. Cell lysates were run on an SDS denaturing gel, transferred to a nitrocellulose membrane, and immunoblotted with either anti-IκB-α antibody or anti-phospho-p38 antibody (Cell Signaling Technology). Anti-GAPDH (Advanced Immunochemicals) or anti-total p38 antibodies, respectively, were used to reprobe the membranes to check for equal loading of the gels.

IRAK1 Degradation Assays—Cells were plated in a 6-well plate at a density of 2×10^6 cells/well and stimulated the next day with either PAM_2CSK_4 (10 nM) or R848 (20 μM) for the indicated time intervals. Cell lysates were run on a denaturing gel and Western blotted with anti-IRAK1 antibody (Cell Signaling Technology). GAPDH was used as an internal loading control.

Confocal Microscopy Imaging—HEK293T cells were seeded in 35-mm glass bottom tissue culture dishes (Mat Tek Corporation) at a density of 250,000 cells/dish. Next day, the cells were transiently transfected with the indicated plasmids. Twenty-four hours later, live cells were imaged on a Leica SP2 AOBS confocal laser-scanning microscope. A sequential scan was conducted for co-localization studies to rule out any possibility of cross-talk between the different fluorophores.

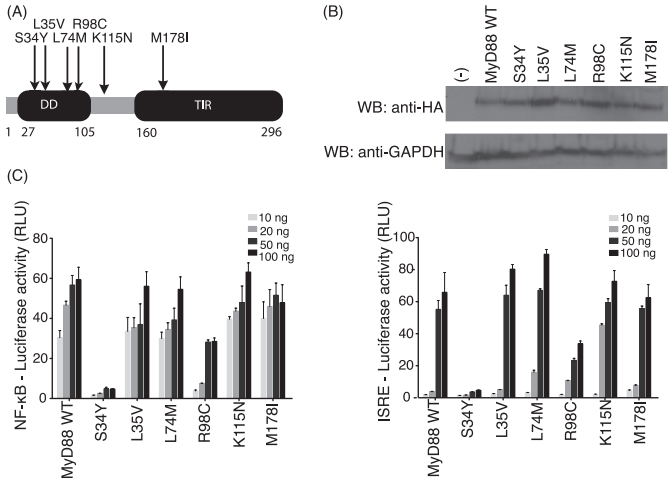

FIGURE 1. **Transient expression of MyD88 S34Y is unable to activate NF-κB and IRF-5 dependent ISRE reporters.** *A*, schematic of MyD88 domain structure depicting the position of the various nonsynonymous SNPs is shown. *B*, HEK293T cells were transfected with HA-tagged versions of either WT MyD88 or the different variants of MyD88, and expression levels were checked using anti-HA antibody. *C*, HEK293T cells were transfected with the indicated MyD88 construct and either NF-κB luciferase (*left*) or ISRE-luciferase + IRF5 (*right*). Twenty-four hours later, luciferase activity was measured in cell lysates. *Renilla* luciferase values were used to normalize for transfection efficiency. Results are reported as a mean of triplicate determinations ± S.D. (*error bars*). The graphs are a representative of three (*left*) or two (*right*) independent experiments. *DD*, death domain; *WB*, Western blotting.

Recruitment of MyD88 to Cell Membrane—A MyD88-deficient macrophage-like cell line was infected with retrovirus carrying either MyD88 (WT)-citrine or S34Y-citrine. The positive cells were sorted by flow cytometry and then allowed to recover for 2–3 days. The cells were seeded in 35-mm glass bottom tissue culture dishes at a density of 250,000 cells/dish. The next day, they were stimulated with either LPS (100 ng/ml) or poly(I·C) (20 μg/ml).

Fluorescence Energy Resonance Transfer (FRET)—HEK293T cells were seeded in 35-mm glass bottom tissue culture dishes at a density of 150,000 cells/dish. Next day, the cells were transiently transfected with the indicated plasmids. FRET between the respective proteins was calculated by measuring sensitized emission (SE) fluorescence using the FRET SE wizard on the Leica SP2 confocal laser-scanning microscope. In each case, cerulean-tagged protein acted as the donor fluorophore whereas the citrine-tagged protein functioned as the acceptor fluorophore. Excitation wavelengths for the donor and acceptor were 405 nM and 514 nM, respectively. The FRET efficiency is shown as a color-coded scale of values between 0 and 100%. The average of three selected regions of interest was used to quantitate the FRET efficiency for each sample.

RESULTS

S34Y Overexpression Fails to Activate Both NF-κB and IRF5-dependent ISRE Reporters—Human MyD88 has six nonsynonymous SNPs in its coding region (Fig. 1*A*). When expressed in

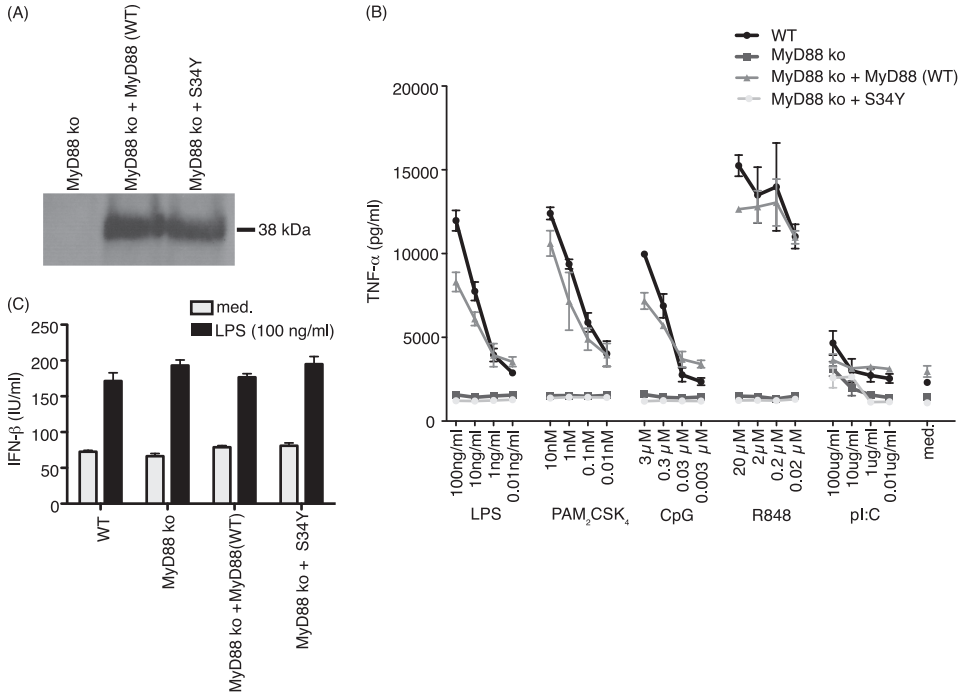

FIGURE 2. **MyD88-deficient macrophages expressing S34Y have impaired cytokine production.** *A*, MyD88-deficient macrophages were infected with an IRES-GFP-expressing retrovirus MSCV2.2, carrying HA-tagged versions of either WT MyD88 or the mutant S34Y. The positive cells were sorted based on GFP expression, and the expression levels of the proteins were checked using an anti-HA antibody. *B*, cells were stimulated overnight with the indicated TLR ligands, and the levels of TNF-α in the culture supernatants were analyzed by ELISA. Results are reported as a mean of triplicate determinations ± S.D. (*error bars*). The graph is a representative of three independent experiments. *C*, same supernatants (only LPS stimulation) were analyzed for IFN-β levels by ELISA. Results are reported as a mean of triplicate determinations ± S.D. The graph is a representative of three independent experiments.

HEK293T cells, all mutants are expressed at levels similar to WT MyD88 (Fig. 1*B*), indicating no intrinsic protein stability defect. To identify variants with altered function, we initially screened all known SNPs in NF-κB reporter assays in HEK293T cells. WT MyD88, when overexpressed, can drive the NF-κB reporter by itself. As evident in Fig. 1*C* (*left panel*), most MyD88 variants exhibited activity comparable with (L35V, L74M, K115N, V178I) or slightly reduced from (R98C) that of WT MyD88. One of the variants, S34Y, however, was completely inactive in driving the NF-κB reporter. Additionally, we tested the activity of the MyD88 variants in IRF5-mediated ISRE luciferase reporter assays. IRF5 is a transcription factor whose activation is dependent on MyD88. Similar to the NF-κB luciferase assay, WT MyD88 and all variants except S34Y were able to activate the ISRE reporter (Fig. 1*C*, *right panel*). S34Y was completely compromised in its ability to drive the ISRE luciferase reporter.

S34Y Is Unable to Restore Function in Immortalized MyD88-deficient Macrophage-like Cell Line—To study these polymorphisms in a MyD88-deficient background, we transduced an immortalized MyD88-deficient macrophage cell line (17) with a retrovirus MSCV2.2 (15) carrying an HA-tagged version of either WT MyD88 or S34Y. This retrovirus transcribes GFP from an IRES element, thus making the positively transduced cells fluorescent. Western blotting with an anti-HA antibody confirmed comparable levels of expression of WT MyD88 and S34Y (Fig. 2*A*). When stimulated with the different TLR ligands, immortalized WT cells responded to all the tested ligands (Fig. 2*B*) and secreted appreciable amounts of the cytokine TNF-α. On the other hand, MyD88 knock-out cells could not mount a response to any ligand (LPS, PAM_2CSK_4, CpG, or R848) except poly(I·C), which is a TLR3 ligand and signals independently of MyD88. As expected, MyD88 knock-out cells expressing WT MyD88 behaved just like the WT cell line and responded to all ligands (Fig. 2*B*). In contrast, cytokine production in cells expressing S34Y was completely ablated when stimulated with any of the MyD88-dependent ligands. They could, however, respond just as well as the other cell lines to the TLR3 ligand poly(I·C). A similar pattern was seen in the case of another proinflammatory cytokine, IL-6 (data not shown). To test whether MyD88-independent pathways are functional in S34Y-expressing cells, we measured IFN-β production upon LPS stimulation, which is mediated primarily by the adapter TRIF. The cells expressing the mutant S34Y were able to produce IFN-β at levels similar to WT cells (Fig. 2*C*). Hence, S34Y impairs only MyD88-dependent TLR signaling, whereas cytokine production by MyD88-independent pathways remains unaffected.

NF-κB and MAPK (p38) Activation Is Impaired in Macrophages That Express MyD88 S34Y—TLR engagement leads to the activation of a variety of transcription factors like NF-κB, AP-1, and IRFs (19), as well as mitogen-activated protein kinases (MAPKs) (20), although NF-κB is the predominant transcription factor involved in MyD88-dependent signaling. IκB-α is the inhibitor of NF-κB, and its degradation via ubiquitination implies activation of NF-κB. We thus tested the activation status of NF-κB in the cell lines expressing WT MyD88 or S34Y. Immortalized WT, MyD88-deficient, MyD88-deficient cells expressing WT MyD88 or S34Y were stimulated with either PAM_2CSK_4 (a TLR2 ligand) or R848 (a TLR7 ligand).

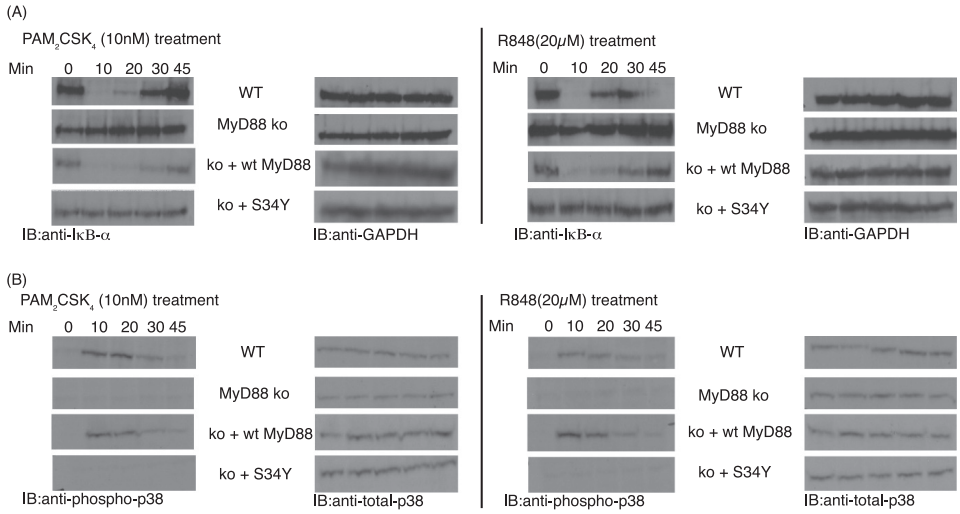

FIGURE 3. **IκB degradation and MAPK (p38) activation are impaired in macrophages that express MyD88 S34Y.** *A*, NF-κB activation was examined by assessing IκB degradation. Cells were plated in a 6-well plate and stimulated with either 10 nM PAM_2CSK_4 or 20 μM R848 for the indicated time intervals. Cell lysates were made, run on a gel, transferred to nitrocellulose membrane, and blotted (*IB*) with an anti-IκB antibody. GAPDH levels served as an internal loading control. *B*, same cell lysates were also analyzed for p38 MAPK activation by examining phosphorylation of p38 using anti-pp38 antibody. Total p38 MAPK levels acted as an internal loading control.

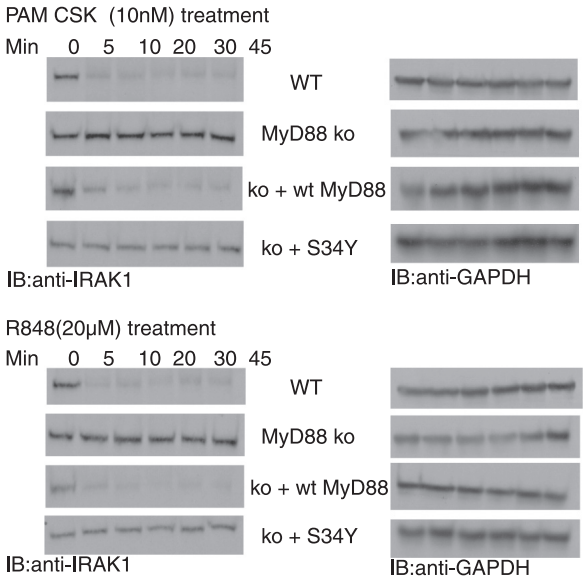

FIGURE 4. **Macrophages expressing S34Y are unable to degrade IRAK1 effectively.** IRAK1 degradation was examined in the reconstituted cell lines as a marker of an active signal complex formation. Cells were plated in a 6-well plate and stimulated with either 10 nM PAM_2CSK_4 or 20 μM R848 for the indicated time intervals. Cell lysates were made, run on a gel, transferred to nitrocellulose membrane, and blotted (*IB*) with an anti-IRAK1 antibody. GAPDH levels served as an internal loading control.

These two ligands were selected based on the localization pattern of their receptors. TLR2 is a cell membrane receptor, whereas TLR7 is an endosomal TLR. Thus, using these ligands gives a complete picture of MyD88-dependent signaling from both sites: cell surface as well as the endosome. The immortalized WT cells responded to both PAM_2CSK_4 and R848 and could degrade IκB-α starting as early as 10 min (Fig. 3*A*). MyD88-deficient cells, however, did not respond to either ligand, and we could see no degradation of IκB-α in these cells. The cells expressing WT MyD88 behaved like the WT macrophages and could degrade IκB-α starting at 10 min. On the other hand, the cells expressing S34Y were completely deficient in their ability to degrade IκB-α when stimulated with either PAM_2CSK_4 or R848 (Fig. 3*A*).

Having demonstrated that S34Y-expressing cells exhibit impaired NF-κB activation, we wondered whether this defect in response included impaired MAPK activation. We selected p38 MAPK as a prototype of MAPK activation and examined its phosphorylation status as a marker for its activation. Phosphorylation of p38 MAPK followed the same pattern as NF-κB activation, and S34Y-expressing cells did not phosphorylate p38 upon stimulation with either PAM_2CSK_4 or R848 (Fig. 3*B*). Thus, S34Y is a nonfunctional mutation that renders MyD88 completely defective in signaling.

Signaling through MyD88 S34Y Does Not Lead to the Formation of a Functional Signaling Complex—Once a TLR is activated by its respective ligand, MyD88 recruits IRAK1 and IRAK4 to the receptor complex through death domain interactions. IRAK4 then phosphorylates and activates IRAK1, which can then autophosphorylate itself. This hyperphosphorylated form of IRAK1 then undergoes ubiquitination-mediated degradation (21, 22). These phosphorylation and degradation events are thus hallmarks of an active signal transduction pathway.

We initially hypothesized that the S34Y mutant MyD88 is unable to bind either IRAK1 or IRAK4. However, co-immunoprecipitation assays in HEK293T cells revealed that the presence of the S34Y mutation does not affect the ability of MyD88 to bind either IRAK1 or IRAK4 (data not shown). We thus tested whether the activation signal is effectively relayed to the downstream effectors by analyzing the degradation of IRAK1. Treatment with either PAM_2CSK_4 or R848 results in degradation of IRAK1 as early as 5 min, in the WT immortalized cells (Fig. 4). As expected, the MyD88-deficient cells are not able to form an active signalosome and hence cannot degrade IRAK1. MyD88-deficient cells expressing WT MyD88 behaved similarly to WT cells and could respond to both of the tested ligands. The cells expressing S34Y, however, were unable to degrade IRAK1 upon stimulation with PAM_2CSK_4 or R848. Hence, even though MyD88 S34Y is able to interact with IRAK4

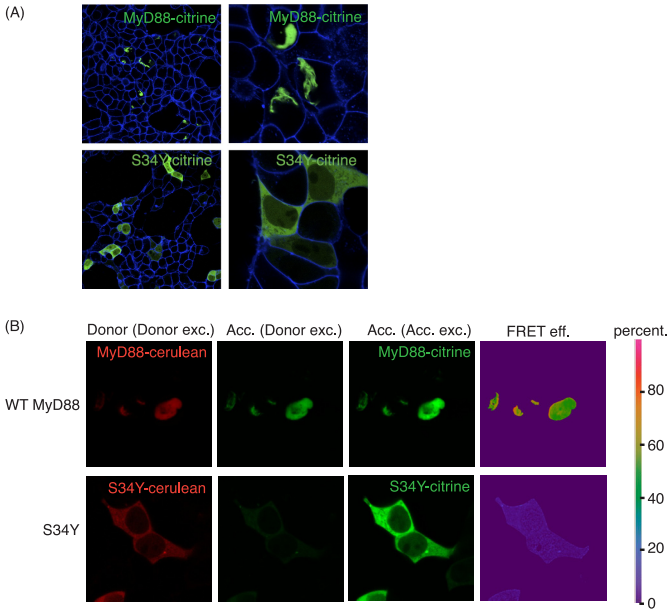

FIGURE 5. **Unlike WT MyD88, S34Y does not form oligomeric aggregates.** *A*, citrine-tagged WT MyD88 or S34Y (*green*) was transfected into HEK293T cells. The next day, live cells were imaged using standard confocal procedures. *B*, HEK293T cells were transiently transfected with the indicated plasmids. FRET between cerulean- and citrine-tagged WT MyD88 or cerulean- and citrine-tagged S34Y was calculated by measuring SE fluorescence using FRET SE wizard on the Leica SP2 confocal laser-scanning microscope. The FRET efficiency is shown as a *color-coded scale* of values between 0 and 100%.

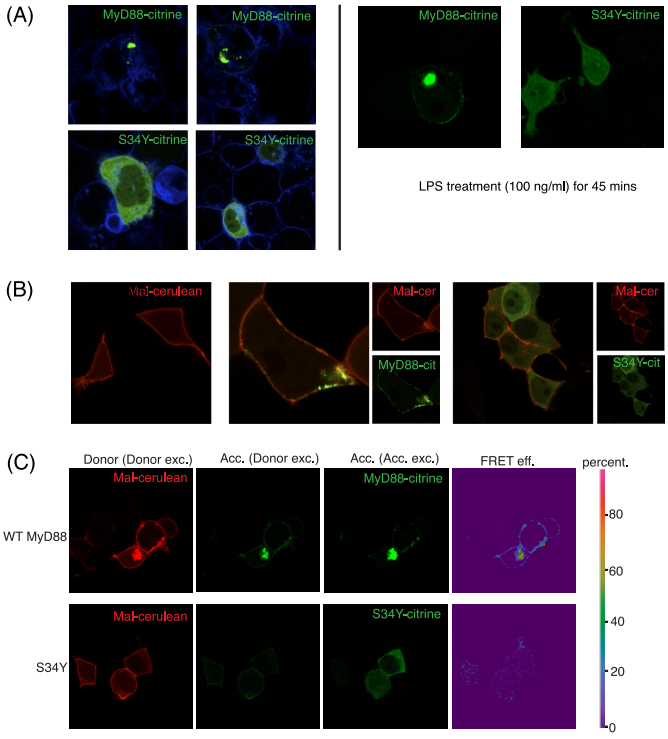

FIGURE 6. **S34Y does not traffic to the cell membrane.** *A*, macrophages expressing either citrine-tagged MyD88 WT or S34Y were imaged using standard confocal microscopy. The cells were either left untreated (*left panel*) or stimulated with LPS (100 ng/ml) for 45 min (*right panel*). *B*, HEK293T cells were transfected with cerulean-tagged Mal either by itself or in conjunction with citrine-tagged WT MyD88 or S34Y. The next day the cells were imaged using standard confocal microscopy procedures. *C*, HEK293T cells were transiently transfected with the indicated plasmids. FRET between Mal and WT MyD88 or S34Y was calculated by measuring SE fluorescence using FRET SE wizard on the Leica SP2 confocal laser-scanning microscope. The FRET efficiency is shown as a *color-coded scale* of values between 0 and 100%.

and IRAK1, these interactions are not functional or occur at a level that is much reduced compared with WT MyD88 (as immunoprecipitation assays are not reliably quantitative), and thus the activation signal is not conveyed to the downstream effectors.

Having shown that MyD88 S34Y is completely defective in signaling through the TLRs, we next sought an explanation for this phenotype. Co-immunoprecipitation assays in HEK293T cells did not reveal a defect in the ability of MyD88 S34Y to interact with any of the known binding partners of MyD88 (data not shown).

S34Y Has a Different Localization Pattern than WT MyD88—Because the S34Y mutation did not seem to affect any interactions, we next tested whether MyD88 S34Y has a localization pattern different from that of WT MyD88. In 1998, Jaunin *et al.* demonstrated that WT MyD88, when expressed in HeLa cells, is localized in fibrillar aggregates (23). A number of other groups reported similar findings, including our own group (24, 25). Indeed, we found that when citrine-tagged WT MyD88 was expressed in HEK293T cells, it localized to aggregates or distinct foci in the cytoplasm, with almost no diffuse cytoplasmic expression (Fig. 5*A*, *upper panels*). S34Y, however, was completely diffuse in the cytoplasm, with no aggregate structures (Fig. 5*A*, *lower panels*). To confirm that the aggregates we see in the case of WT MyD88 are indeed oligomeric complexes of MyD88, we carried out FRET analysis with cerulean- and citrine-tagged MyD88 (WT). Both cerulean- and citrine-tagged MyD88 localized to the condensed structures in the cell, and a very strong FRET signal could be observed between the two differentially tagged WT MyD88s (Fig. 5*B*). In contrast, cerulean and citrine-tagged S34Y co-localized in the cytoplasm with a complete absence of aggregates. In this case, the FRET efficiency was significantly lower than the WT experimental set, thus demonstrating that the S34Y mutation affects the ability of MyD88 to form its own oligomeric complexes.

Some recent studies suggest that the activity/function of MyD88 might be related to its correct subcellular targeting or the ability to aggregate in the cytoplasm. A study by Nishiya *et al.* demonstrated that the signaling function of MyD88 is dependent on its correct cellular localization, and the entire non-TIR region of MyD88 is responsible for its correct localization (26). They further show that the deletions or truncations in this region that change the localization of MyD88, making it diffusely expressed in the cytoplasm, also render MyD88 inactive in NF-κB reporter assays. Hence, in accordance with previously published reports, we show that proper localization of MyD88 is indispensable for its function. In addition, we show that a naturally occurring loss-of-function mutation of MyD88 changes the subcellular localization of MyD88.

S34Y Does Not Traffic to the Cell Membrane—When citrine-tagged MyD88 (WT) or S34Y is expressed in MyD88-deficient macrophages, they both retain their characteristic localization pattern. WT MyD88 is present in condensed aggregates whereas S34Y is diffused cytoplasmic (Fig. 6*A*, *left panel*). To investigate ligand-dependent MyD88 recruitment to the site of activation, we stimulated the cells with the TLR4 ligand, LPS.

Forty-five minutes after stimulation, MyD88 could be observed at the cell membrane (Fig. 6*A*, *right panel*). This mobilization of MyD88 requires activation by a MyD88-dependent ligand, as poly(I·C), a TLR3 ligand, failed to induce mobilization (data not shown). However, no change could be observed in S34Y-expressing cells. LPS stimulation did not lead to S34Y trafficking to the membrane (Fig. 6*A*, *right panel*).

We also tested the co-localization of MyD88/S34Y with the adapter Mal. When WT MyD88 is co-expressed with Mal/TIRAP, it relocalizes from the condensed foci to the cell membrane where it co-localizes with Mal (25). We had similar observations when we transiently transfected Mal-cerulean with WT MyD88-citrine. Instead of being localized to distinct foci in the cytoplasm, MyD88 was co-localized at the cell membrane with Mal (Fig. 6*B*). As a control, we co-expressed Mal D96N with WT MyD88. Mal D96N is a naturally occurring mutation of Mal that interferes with MyD88 binding (27). As expected, Mal D96N was unable to traffic WT MyD88 to the membrane (data not shown). In the case of S34Y, co-expressed with Mal, S34Y retained its diffuse cytoplasmic expression and did not get recruited to the membrane. Because co-immunoprecipitation assays did not reveal a defect in the binding of MyD88 S34Y with Mal, we employed FRET analysis to shed some light on the interactions between Mal and MyD88 S34Y. WT MyD88 and Mal co-expression resulted in a strong FRET signal limited to the cell membrane, the site of interaction (Fig. 6*C*). In contrast, S34Y and Mal generated a comparatively weaker FRET signal, in the cytoplasm. Thus, even though S34Y interacts with Mal in the cytoplasm, it is unable to be recruited to the membrane, the functional site for Mal- and MyD88-dependent receptor activation. The recruitment of WT MyD88 but not S34Y to the membrane illustrates the fact that the observed aggregates of MyD88 are functional oligomers and not merely an artifact of overexpression.

MyD88 S34Y Fails to Assemble into Myddosomes—Recently, the crystal structure of the MyD88-IRAK4-IRAK1 death domain complex has been determined (2). These three proteins are present in a ternary complex consisting of six MyD88, four IRAK4, and four IRAK2 death domains. These oligomeric structures have been named "Myddosomes" by the authors. We hypothesized that the foci that WT MyD88 seems to localize to (Fig. 5*A*) may be Myddosomes, and the S34Y mutation ablates the ability of MyD88 to form these oligomeric structures. According to Lin *et al.*, the assembly of the Myddosome is a sequential process (2). Although the MyD88 death domain by itself is able to form oligomers at high concentration, IRAK4 and IRAK2 death domains are monomeric in solution. However, in the presence of MyD88, IRAK4 is oligomerized and forms a complex with oligomeric MyD88. This then acts as a platform for recruitment of IRAK2 and IRAK1. The authors believe that this hierarchical assembly is essential for bringing the IRAKs into a proper conformation for their phosphorylation and activation (2). In our study, when cerulean-tagged IRAK4 was expressed in HEK293T cells, it was present diffused in the cytoplasm (Fig. 7*Ai*). However, when we co-expressed citrine-tagged WT MyD88, we observed co-localization of IRAK4 with MyD88 in distinct foci which we believe are Myddosomes (Fig. 7*Aii*). In contrast, when MyD88 S34Y was co-expressed with IRAK4, we observed both proteins to co-localize in the cytoplasm and have a diffuse expression pattern (Fig. 7*Aiii*). Similar observations were made for IRAK2 and MyD88 (WT or S34Y) co-localization (data not shown). Thus, in agreement with Lin *et al.*, we show that IRAK4 and IRAK2 co-localize with MyD88 and form Myddosomes. The S34Y mutation abrogates the ability of MyD88 to form these oligomeric structures.

To confirm the formation of a complex between MyD88 and IRAK4, we examined the occurrence of FRET between IRAK4

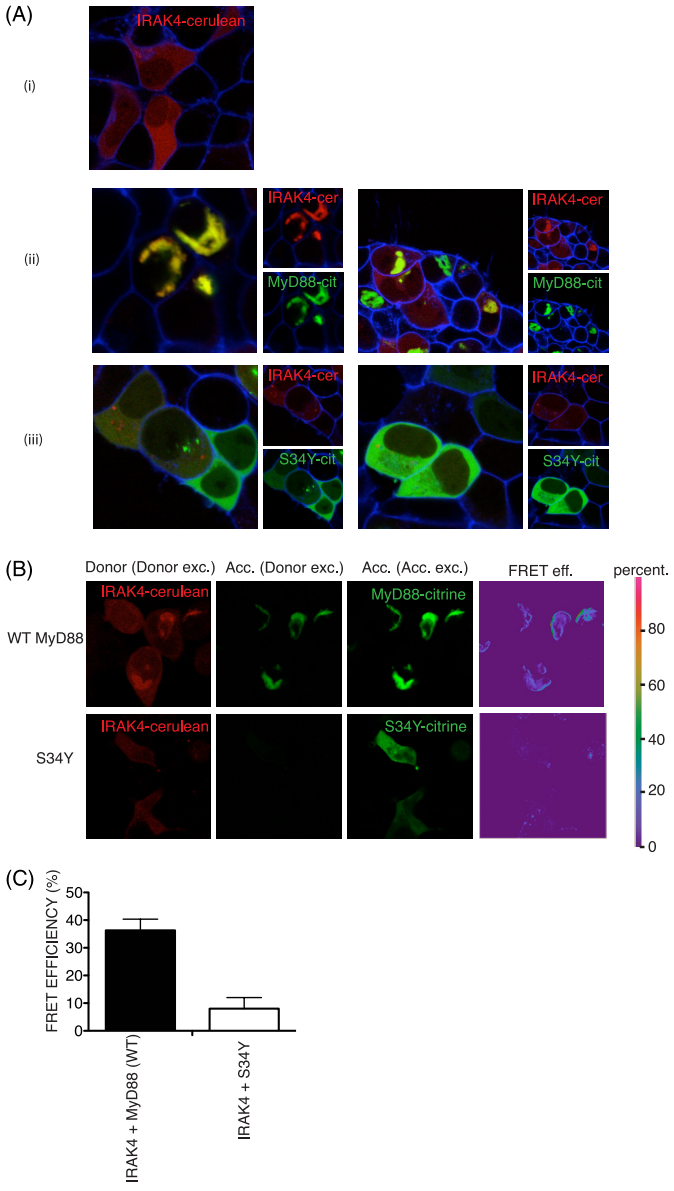

FIGURE 7. **S34Y fails to assemble into a Myddosome.** *A*, cerulean-tagged IRAK4 (*red*) was transfected either by itself (*i*) or in conjunction with citrine-tagged WT MyD88 (*ii*) or S34Y (*iii*) (*green*) into HEK293T cells. The next day, the cells were imaged using sequential scanning, and co-localization of the two proteins was assessed. These images are representative of at least three independent experiments. *B*, HEK293T cells were transiently transfected with the indicated plasmids. FRET between IRAK4 and WT MyD88 or S34Y was calculated by measuring SE fluorescence using FRET SE wizard on the Leica SP2 confocal laser-scanning microscope. The FRET efficiency is shown as a *color-coded scale* of values between 0 and 100%. *C*, FRET efficiency for both the samples (IRAK4-WT MyD88 and IRAK4-S34Y) was obtained by calculating the average efficiency of different regions in each FRET image. This experiment is a representative of two independent experiments.

and WT MyD88. Cerulean-tagged IRAK4 and citrine-tagged MyD88 were used as the donor and acceptor, respectively. A strong FRET signal was detected between IRAK4 and WT MyD88 in the regions of co-localization (Fig. 7*B*, *upper panels*). Three different regions of interest in the FRET efficiency image were selected, and their average was used to denote the FRET efficiency of the sample (Fig. 7*C*). FRET between WT MyD88 and IRAK4 occurred at a very high efficiency of 36%. Because the efficiency of FRET is inversely proportional to the distance between the two participating proteins, such a high FRET signal implies that IRAK4 and WT MyD88 interact strongly with each other and are present in a complex. Similar FRET experiments with the mutant MyD88 S34Y, however, yielded quite a low FRET signal (Fig. 7*B*, *lower panels*) with an average efficiency of 8% (Fig. 7*C*), suggesting that though both IRAK4 and S34Y are present diffused in the cytoplasm, they are not in close proximity and do not form a functional complex, required for the function of MyD88.

DISCUSSION

TLRs are critical for mounting an effective immune response against invading pathogens. The signaling cascade that ensues upon ligand recognition is marked by finely orchestrated molecular interactions between the receptor and the adapters, as well as various downstream kinases and effector molecules. SNPs in the coding regions of proteins involved in such a signaling pathway can sometimes alter the functional properties of the protein, thus affecting the outcome of the signal transduction pathway. Human MyD88 has six nonsynonymous SNPs in its coding region, making it one of the most polymorphic TLR adapter proteins. However, the effect of these SNPs on the function of MyD88 remains poorly understood. In our study, we have screened these SNPs with the hypothesis that some of them may alter the signaling potential of MyD88. We report that one of the polymorphisms, S34Y, which lies in the death domain of MyD88, is a complete loss-of-function variant of MyD88. Of note, we did not observe a dramatic phenotype in MyD88 R98C, in contrast to results reported elsewhere (28).

Cellular biological studies of signaling molecules are typically done in easily transfectable cells, like HEK293T, which have little in common with the innate immune cells they are thought to represent. Typically, studies in HEK293T cells are inherently compromised due to the presence of the WT alleles. Using immortalized macrophages from MyD88 knock-out animals, we have successfully reconstituted both fully functional macrophage cell lines and mutant macrophage lines using viral expression systems. These extensive studies have shown that effector cells are extraordinarily destabilized by both the absence of MyD88 (as would have been predicted) and by S34Y. Indeed, some of the most important effector functions, in addition to the activation of NF-κB and its associated downstream genes (such as TNF-α), were clearly compromised by the expression of S34Y, including p38 activation downstream from TLRs 2 and 7. When one takes into account the variety of immune defects that we have documented in macrophages expressing S34Y, it is no surprise that S34Y appears to be a rare mutation, rather than a true "polymorphism," and is similar in incidence to MyD88 deficiency (11). Indeed, we screened 267 samples from healthy individuals and 105 DNA samples from children with meningococcal sepsis and failed to find a single individual in either group with even a single mutant allele (data not shown). Although knock-out mice with MyD88 deficiency seem to survive well in our "clean" animal facilities, there seems to be little question that in real life, functional MyD88 is a necessity.

The death domain (and the intervening region between the death and TIR domains) of MyD88 has earlier been implicated in the proper localization of MyD88 (26). Nishiya *et al.* demonstrated that the entire non-TIR region of MyD88 is important to maintain the distinct and condensed pattern of MyD88 localization. In fact, there have been other reports that illustrate similar findings, that indeed MyD88 is present in aggregate structures in the cytoplasm (23, 25). Furthermore, this seems to be a characteristic of MyD88 that is conserved across species (29). A recent study by Liu *et al.* show that zebrafish MyD88 is also expressed as large condensed spots in the cytoplasm of cells, and this observation is reproducible in different cell lines. Moreover, there seems to be a correlation between the localization and function of MyD88. Both Nishiya *et al.* and Liu *et al.* find that deletions or mutations that change the expression pattern of MyD88 from condensed spots to diffuse cytoplasmic localization also affect the function of MyD88, making it inactive in signaling. In view of all these studies, we compared the localization pattern of WT MyD88 and the variant S34Y. As expected, WT MyD88 was localized to large condensed spots, in the cytoplasm. However, S34Y had a completely different pattern of expression. It was present diffused in the cytoplasm and did not form any aggregates.

The condensed spots that MyD88 seems to localize to have as yet not been associated with any subcellular organelle or structure. In light of the report by Lin *et al.* we propose that these aggregate structures are Myddosomes, helical oligomers of MyD88, IRAK4, and IRAK2 or MyD88, IRAK4, and IRAK1. However, there is currently no method to study the exact stoichiometry of IRAK4/IRAK2/MyD88 aggregates inside the cell, and hence we cannot formally demonstrate that these aggregates are Myddosomes. The presence of fluorescent oligomers is reminiscent of the ability to view other large protein assemblies devoted to innate immunity, such as the ability to view pyroptosome formation using fluorescent constructs of ASC that are expressed in the presence of an NLR and caspase 1 (the so-called "speckle" assay) (30). Consistent with the findings by Lin *et al.* we show that MyD88 by itself is present in aggregates whereas IRAK4 is diffusely expressed in the cytoplasm. However, on co-expressing them, IRAK4 co-localizes to these distinct foci along with MyD88. Most importantly, the mutant MyD88 S34Y is unable to form Myddosomes with IRAK4. The crystal structure of the Myddosomes resolved by Lin *et al.* used just the death domains of the three proteins involved. We, on the other hand, have employed full-length proteins in all our studies and show for the first time the formation of Myddosomes in cells. More importantly, we identify a natural loss of function mutation in MyD88 that disrupts its ability to form Myddosomes.

REFERENCES

1. Kawai, T., and Akira, S. (2010) *Nat. Immunol.* **11,** 373–384
2. Lin, S. C., Lo, Y. C., and Wu, H. (2010) *Nature* **465,** 885–890
3. Akahoshi, M., Nakashima, H., Sadanaga, A., Miyake, K., Obara, K., Tamari, M., Hirota, T., Matsuda, A., and Shirakawa, T. (2008) *Lupus* **17,** 568–574
4. De Jager, P. L., Richardson, A., Vyse, T. J., and Rioux, J. D. (2006) *Arthritis Rheum.* **54,** 1279–1282
5. Hamann, L., Glaeser, C., Hamprecht, A., Gross, M., Gomma, A., and Schumann, R. R. (2006) *Clin. Chim. Acta* **364,** 303–307
6. Mockenhaupt, F. P., Cramer, J. P., Hamann, L., Stegemann, M. S., Eckert, J., Oh, N. R., Otchwemah, R. N., Dietz, E., Ehrhardt, S., Schröder, N. W., Bienzle, U., and Schumann, R. R. (2006) *Proc. Natl. Acad. Sci. U.S.A.* **103,** 177–182
7. Texereau, J., Chiche, J. D., Taylor, W., Choukroun, G., Comba, B., and Mira, J. P. (2005) *Clin. Infect. Dis.* **41,** S408–415
8. Ferwerda, B., Alonso, S., Banahan, K., McCall, M. B., Giamarellos-Bourboulis, E. J., Ramakers, B. P., Mouktaroudi, M., Fain, P. R., Izagirre, N., Syafruddin, D., Cristea, T., Mockenhaupt, F. P., Troye-Blomberg, M., Kumpf, O., Maiga, B., Dolo, A., Doumbo, O., Sundaresan, S., Bedu-Addo, G., van Crevel, R., Hamann, L., Oh, D. Y., Schumann, R. R., Joosten, L. A., de la Rúa, C., Sauerwein, R., Drenth, J. P., Kullberg, B. J., van der Ven, A. J., Hill, A. V., Pickkers, P., van der Meer, J. W., O'Neill, L. A., and Netea, M. G. (2009) *Proc. Natl. Acad. Sci. U.S.A.* **106,** 10272–10277
9. Hawn, T. R., Dunstan, S. J., Thwaites, G. E., Simmons, C. P., Thuong, N. T., Lan, N. T., Quy, H. T., Chau, T. T., Hieu, N. T., Rodrigues, S., Janer, M., Zhao, L. P., Hien, T. T., Farrar, J. J., and Aderem, A. (2006) *J. Infect. Dis.* **194,** 1127–1134
10. Khor, C. C., Chapman, S. J., Vannberg, F. O., Dunne, A., Murphy, C., Ling, E. Y., Frodsham, A. J., Walley, A. J., Kyrieleis, O., Khan, A., Aucan, C., Segal, S., Moore, C. E., Knox, K., Campbell, S. J., Lienhardt, C., Scott, A., Aaby, P., Sow, O. Y., Grignani, R. T., Sillah, J., Sirugo, G., Peshu, N., Williams, T. N., Maitland, K., Davies, R. J., Kwiatkowski, D. P., Day, N. P., Yala, D., Crook, D. W., Marsh, K., Berkley, J. A., O'Neill, L. A., and Hill, A. V. (2007) *Nat. Genet.* **39,** 523–528
11. von Bernuth, H., Picard, C., Jin, Z., Pankla, R., Xiao, H., Ku, C. L., Chrabieh, M., Mustapha, I. B., Ghandil, P., Camcioglu, Y., Vasconcelos, J., Sirvent, N., Guedes, M., Vitor, A. B., Herrero-Mata, M. J., Aróstegui, J. I., Rodrigo, C., Alsina, L., Ruiz-Ortiz, E., Juan, M., Fortuny, C., Yagüe, J., Antón, J., Pascal, M., Chang, H. H., Janniere, L., Rose, Y., Garty, B. Z., Chapel, H., Issekutz, A., Maródi, L., Rodriguez-Gallego, C., Banchereau, J., Abel, L., Li, X., Chaussabel, D., Puel, A., and Casanova, J. L. (2008) *Science* **321,** 691–696
12. Sweet, C. R., Conlon, J., Golenbock, D. T., Goguen, J., and Silverman, N. (2007) *Cell. Microbiol.* **9,** 2700–2715
13. Schoenemeyer, A., Barnes, B. J., Mancl, M. E., Latz, E., Goutagny, N., Pitha, P. M., Fitzgerald, K. A., and Golenbock, D. T. (2005) *J. Biol. Chem.* **280,** 17005–17012
14. Fitzgerald, K. A., Rowe, D. C., Barnes, B. J., Caffrey, D. R., Visintin, A., Latz, E., Monks, B., Pitha, P. M., and Golenbock, D. T. (2003) *J. Exp. Med.* **198,** 1043–1055
15. Hawley, R. G., Lieu, F. H., Fong, A. Z., and Hawley, T. S. (1994) *Gene. Ther.* **1,** 136–138
16. Melo, M. B., Kasperkovitz, P., Cerny, A., Könen-Waisman, S., Kurt-Jones, E. A., Lien, E., Beutler, B., Howard, J. C., Golenbock, D. T., and Gazzinelli, R. T. (2010) *PLoS Pathog.* **6,** e1001071
17. Sheedy, F. J., Palsson-McDermott, E., Hennessy, E. J., Martin, C., O'Leary, J. J., Ruan, Q., Johnson, D. S., Chen, Y., and O'Neill, L. A. (2010) *Nat. Immunol.* **11,** 141–147
18. Roberts, Z. J., Goutagny, N., Perera, P. Y., Kato, H., Kumar, H., Kawai, T., Akira, S., Savan, R., van Echo, D., Fitzgerald, K. A., Young, H. A., Ching, L. M., and Vogel, S. N. (2007) *J. Exp. Med.* **204,** 1559–1569
19. Kawai, T., and Akira, S. (2007) *Trends Mol. Med.* **13,** 460–469
20. Dong, C., Davis, R. J., and Flavell, R. A. (2002) *Annu. Rev. Immunol.* **20,** 55–72
21. Gottipati, S., Rao, N. L., and Fung-Leung, W. P. (2008) *Cell. Signal.* **20,** 269–276
22. Yamin, T. T., and Miller, D. K. (1997) *J. Biol. Chem.* **272,** 21540–21547
23. Jaunin, F., Burns, K., Tschopp, J., Martin, T. E., and Fakan, S. (1998) *Exp. Cell. Res.* **243,** 67–75
24. Latz, E., Visintin, A., Lien, E., Fitzgerald, K. A., Monks, B. G., Kurt-Jones, E. A., Golenbock, D. T., and Espevik, T. (2002) *J. Biol. Chem.* **277,** 47834–47843
25. Kagan, J. C., and Medzhitov, R. (2006) *Cell* **125,** 943–955
26. Nishiya, T., Kajita, E., Horinouchi, T., Nishimoto, A., and Miwa, S. (2007) *FEBS Lett.* **581,** 3223–3229
27. Nagpal, K., Plantinga, T. S., Wong, J., Monks, B. G., Gay, N. J., Netea, M. G., Fitzgerald, K. A., and Golenbock, D. T. (2009) *J. Biol. Chem.* **284,** 25742–25748
28. George, J., Motshwene, P. G., Wang, H., Kubarenko, A. V., Rautanen, A., Mills, T. C., Hill, A. V., Gay, N. J., and Weber, A. N. (2011) *J. Biol. Chem.* **286,** 1341–1353
29. Liu, Y., Li, M., Fan, S., Lin, Y., Lin, B., Luo, F., Zhang, C., Chen, S., Li, Y., and Xu, A. (2010) *J. Immunol.* **185,** 3391–3400
30. Halle, A., Hornung, V., Petzold, G. C., Stewart, C. R., Monks, B. G., Reinheckel, T., Fitzgerald, K. A., Latz, E., Moore, K. J., and Golenbock, D. T. (2008) *Nat. Immunol.* **9,** 857–865